New Journal of Physics
The open–access journal for physics

Nonlinear instability and dynamics of polaritons in quantum systems

P K Shukla[1] **and B Eliasson**
Institut für Theoretische Physik, Ruhr-Universität Bochum, D-44780 Bochum, Germany
E-mail: ps@tp4.rub.de

New Journal of Physics **9** (2007) 98
Received 26 January 2007
Published 20 April 2007
Online at http://www.njp.org/
doi:10.1088/1367-2630/9/4/098

Abstract. We present analytical and simulation studies of the nonlinear instability and dynamics of an electron–hole/anti-electron (hereafter referred to as polaritons) system, which are common in ultra-small devices (semiconductors and micromechanical systems) as well as in dense astrophysical environments and the next generation intense laser–matter interaction experiments. Starting with three coupled nonlinear equations (two Schrödinger equations for interacting polaritons at quantum scales and the Poisson equation determining the electrostatic interactions and the associated charge separation effect), we demonstrate novel modulational instabilities and nonlinear polaritonic structures. It is suggested that the latter can transport information at quantum scales in high-density, ultracold quantum systems.

Phenomena occurring at quantum scales are of paramount importance in diverse areas of physics, and have potential applications in ultra-small devices (e.g. semiconductors and micromechanical systems [1]–[3]), in dense astrophysical environments [4], in intense laser–matter interaction experiments [5], in quantum dots and nanowires [6], in biophotonics [7] and in cool vibes [8]. Quantum mechanical effects (e.g. tunnelling) become important when the de Broglie length is comparable to inter-particle distances in the quantum system. In such a situation, strong correlations among electrons or holes/anti-electrons (hereafter referred to as polaritons) in dense matter produce wavefunction dispersion at quantum scales. In dense quantum systems, the dynamics of polaritons is governed by the Wigner–Poisson (W–P) system that includes the dispersive effects. It turns out that the W–P equations can be represented in the form of generalized quantum hydrodynamic (GQH) equations, which somewhat resemble those describing the dynamics of Bose–Einstein condensates (BECs) in ultracold matter [9]. In quantum systems,

[1] Author to whom any correspondence should be addressed.

PII: S1367-2630(07)42648-9
© IOP Publishing Ltd and Deutsche Physikalische Gesellschaft

the polaritons obey Fermi–Dirac statistics and their dynamics is, in turn, governed by the nonlinear Schrödinger and Poisson equations. The latter are naturally deduced from the GQH equations within the framework of an eikonal representation [10].

Since the polaritons are building blocks of many physical systems as described above, it is timely to present some novel collective interactions involving nonlinear interactions among electrons and holes/anti-electrons in quantum mechanical systems. Specifically, in this paper we present analytical and simulation studies of nonlinearly interacting polaritons and demonstrate the possibility of a new class of modulational instabilities and localized nonlinear structures (bright and dark envelope excitations and quantum vortex pairs). The latter may be exploited to transport information at quantum scales in semiconductors and micromechanical systems.

Let us first present the mathematical model which governs the dynamics of a polariton system. The collective motion of the particles is in this model described by effective Schrödinger equations [10] for the electrons and holes/anti-electrons (denoted by the subscript 'e' and 'h', respectively), coupled with the Poisson equation,

$$\mathrm{i}\hbar\frac{\partial\psi_\mathrm{e}}{\partial t}+\frac{\hbar^2}{2m_\mathrm{e}}\nabla^2\psi_\mathrm{e}+e\phi\psi_\mathrm{e}-W_\mathrm{e}\psi_\mathrm{e}=0, \tag{1}$$

$$\mathrm{i}\hbar\frac{\partial\psi_\mathrm{h}}{\partial t}+\frac{\hbar^2}{2m_\mathrm{h}}\nabla^2\psi_\mathrm{h}-e\phi\psi_\mathrm{h}-W_\mathrm{h}\psi_\mathrm{h}=0, \tag{2}$$

$$\nabla^2\phi=4\pi e(|\psi_\mathrm{e}|^2-|\psi_\mathrm{h}|^2), \tag{3}$$

where $W_\mathrm{e}=m_\mathrm{e}v_\mathrm{Fe}^2|\psi_\mathrm{e}|^{4/D}/2n_0^{2/D}$ and $W_\mathrm{h}=m_\mathrm{h}v_\mathrm{Fh}^2|\psi_\mathrm{h}|^{4/D}/2n_0^{2/D}$ are the pressure terms due to the Fermi temperature of the electrons and holes/anti-electrons, respectively. Furthermore, $v_\mathrm{Fe}=(T_\mathrm{Fe}/m_\mathrm{e})^{1/2}$ and $v_\mathrm{Fh}=(T_\mathrm{Fh}/m_\mathrm{h})^{1/2}$ are the Fermi speeds and $T_\mathrm{Fe}\sim\hbar^2n_0^{2/3}/m_\mathrm{e}$ and $T_\mathrm{Fh}\sim\hbar^2n_0^{2/3}/m_\mathrm{h}$ are the Fermi temperatures of the electrons and holes, and D is the number of spatial dimensions, m_e (m_h) is the effective mass of the electron (hole), and n_0 is the equilibrium electron and hole number density. Hence, we have $|\psi_\mathrm{e}|=|\psi_\mathrm{h}|=n_0^{1/2}$ at equilibrium.

The system of equations (1)–(3) conserves the number of electrons and holes, $N_\mathrm{e}=\int|\psi_\mathrm{e}|^2\,\mathrm{d}^3x$ and $N_\mathrm{h}=\int|\psi_\mathrm{h}|^2\,\mathrm{d}^3x$, respectively, the total momentum $\mathbf{P}=-\mathrm{i}\hbar\int(\psi_\mathrm{e}^*\nabla\psi_\mathrm{e}+\psi_\mathrm{h}^*\nabla\psi_\mathrm{h})\,\mathrm{d}^3x$, the total angular momentum $\mathbf{L}=-\mathrm{i}\hbar\int(\psi_\mathrm{e}^*\mathbf{r}\times\nabla\psi_\mathrm{e}+\psi_\mathrm{h}^*\mathbf{r}\times\nabla\psi_\mathrm{h})\,\mathrm{d}^3x$, and the total energy $\mathcal{E}=\int[-\hbar^2\psi_\mathrm{e}^*\nabla^2\psi_\mathrm{e}/2m_\mathrm{e}-\hbar^2\psi_\mathrm{h}^*\nabla^2\psi_\mathrm{h}/2m_\mathrm{h}+|\nabla\phi|^2/8\pi+D(W_\mathrm{e}|\psi_\mathrm{e}|^2+W_\mathrm{h}|\psi_\mathrm{h}|^2)/(2+D)]\,\mathrm{d}^3x$. The total energy has been obtained from equations (1) and (2) by using the identity $\partial\nabla\phi/\partial t=2\pi\mathrm{i}e\hbar[(\psi_\mathrm{h}\nabla\psi_\mathrm{h}^*-\psi_\mathrm{h}^*\nabla\psi_\mathrm{h})/m_\mathrm{h}-(\psi_\mathrm{e}\nabla\psi_\mathrm{e}^*-\psi_\mathrm{e}^*\nabla\psi_\mathrm{e})/m_\mathrm{e}]$, which is equivalent to the Poisson equation (3).

For the numerical analysis, it is convenient to introduce normalized variables so that a set of key parameters can be identified. Hence, normalizing the wavefunctions ψ_e and ψ_h by $n_0^{1/2}$, the potential ϕ by T_Fe/e, the time t by the Fermi time $t_\mathrm{F}=\hbar/T_\mathrm{Fe}$, and the space $\mathbf{r}$ by the Fermi radius $\lambda_\mathrm{F}=(T_\mathrm{Fe}/4\pi n_0e^2)^{1/2}$, one obtains from (1)–(3) the normalized set of equations $\mathrm{i}\partial\psi_\mathrm{e}/\partial t+A_\mathrm{e}\nabla^2\psi_\mathrm{e}+\phi\psi_\mathrm{e}-|\psi_\mathrm{e}|^{4/D}\psi_\mathrm{e}=0$, $\mathrm{i}\partial\psi_\mathrm{h}/\partial t+(m_\mathrm{e}/m_\mathrm{h})A_\mathrm{e}\nabla^2\psi_\mathrm{h}-\phi\psi_\mathrm{h}-(m_\mathrm{e}/m_\mathrm{h})|\psi_\mathrm{h}|^{4/D}=0$, and $\nabla^2\phi=|\psi_\mathrm{e}|^2-|\psi_\mathrm{h}|^2$, where we identify the parameters $m_\mathrm{h}/m_\mathrm{e}$ and the quantum coupling constant $A_\mathrm{e}=2\pi e^2m_\mathrm{e}/\hbar^2n_0^{1/3}$. These parameters are given in the numerical treatment below.

We next consider the stability of the system (1)–(3). Using the Fourier decomposition

$$\psi_{\rm e} = [\psi_{\rm e0} + \psi_{\rm e+}\exp({\rm i}\mathbf{K}\cdot\mathbf{r} - {\rm i}\Omega t) + \psi_{\rm e-}\exp(-{\rm i}\mathbf{K}\cdot\mathbf{r} + {\rm i}\Omega t)]\exp({\rm i}\mathbf{K}_{e0}\cdot\mathbf{r} - {\rm i}\omega_{\rm e0}t), \tag{4}$$

$$\psi_{\rm h} = [\psi_{\rm h0} + \psi_{\rm h+}\exp({\rm i}\mathbf{K}\cdot\mathbf{r} - {\rm i}\Omega t) + \psi_{\rm h-}\exp(-{\rm i}\mathbf{K}\cdot\mathbf{r} + {\rm i}\Omega t)]\exp({\rm i}\mathbf{K}_{\rm h0}\cdot\mathbf{r} - {\rm i}\omega_{\rm h0}{\rm t}), \tag{5}$$

$$\phi = \widehat{\phi}\exp({\rm i}\mathbf{K}\cdot\mathbf{r} - {\rm i}\Omega t) + \widehat{\phi}^{*}\exp(-{\rm i}\mathbf{K}\cdot\mathbf{r} + {\rm i}\Omega t), \tag{6}$$

in (1)–(3), where $\psi_{\rm e0}$ and $\psi_{\rm h0}$ are the envelopes of the equilibrium electron and hole wavefunctions and $\psi_{\rm e\pm}$, $\psi_{\rm h\pm}$ ($|\psi_{\rm e\pm}|$, $|\psi_{\rm h\pm}| \ll |\psi_{\rm e0}|$, $|\psi_{\rm h0}|$) and $\widehat{\phi}$ are the envelopes of the small-amplitude perturbations of the wavefunctions and potential, respectively, and sorting the equations by different Fourier components, we have the dispersion relations for the electron and hole zeroth order wavefunctions $\hbar\omega_{\rm e0} - \hbar^2 k_{\rm e0}^2/2m_{\rm e} - m_{\rm e}v_{\rm Fe}^2|\psi_{\rm e0}|^{4/D}/2n_0^{2/D} = 0$ and $\hbar\omega_{\rm h0} - \hbar^2 k_{\rm h0}^2/2m_{\rm h} - m_{\rm h}v_{\rm Fh}^2|\psi_{\rm h0}|^{4/D}/2n_0^{2/D} = 0$. We note from equation (3) that $|\psi_{\rm e0}| = |\psi_{\rm h0}|$ $(= n_0^{1/2})$. The nonlinear dispersion relation for the small-amplitude density modulations is

$$\begin{aligned}(D_{\rm e+}D_{\rm e-} - \gamma_{\rm e}^2|\psi_{\rm e0}|^4)(D_{\rm h+}D_{\rm h-} - \gamma_{\rm h}^2|\psi_{\rm h0}|^4) - \beta^2|\psi_{\rm e0}|^2|\psi_{\rm h0}|^2 \\ \times(D_{\rm e+} + D_{\rm e-} + 2\gamma_{\rm e}|\psi_{\rm e0}|^2)(D_{\rm h+} + D_{\rm h-} + 2\gamma_{\rm h}|\psi_{\rm h0}|^2) = 0,\end{aligned} \tag{7}$$

where we have denoted $\beta = 4\pi e^2/K^2$, $\gamma_{\rm e} = \beta + 2\alpha_{\rm e}|\psi_{\rm e0}|^{4/D-2}/D$, $\gamma_{\rm h} = \beta + 2\alpha_{\rm h}|\psi_{\rm h0}|^{4/D-2}/D$, $\alpha_{\rm e} = m_{\rm e}v_{\rm Fe}^2/2n_0^{2/D}$ and $\alpha_{\rm h} = m_{\rm h}v_{\rm Fh}^2/2n_0^{2/D}$. Here the nonlinear wave modes are characterized by

$$D_{\rm e\pm} = \pm\left(\hbar\Omega + \frac{\hbar^2}{m_{\rm e}}\mathbf{K}_{\rm e0}\cdot\mathbf{K}\right) - \frac{\hbar^2K^2}{2m_{\rm e}} - \beta|\psi_{\rm e0}|^2 - \frac{2\alpha_{\rm e}|\psi_{\rm e0}|^{4/D}}{D}, \tag{8}$$

$$D_{\rm h\pm} = \pm\left(\hbar\Omega + \frac{\hbar^2}{m_{\rm h}}\mathbf{K}_{\rm h0}\cdot\mathbf{K}\right) - \frac{\hbar^2K^2}{2m_{\rm h}} - \beta|\psi_{\rm h0}|^2 - \frac{2\alpha_{\rm h}|\psi_{\rm h0}|^{4/D}}{D}. \tag{9}$$

We have solved the dispersion relation (7) numerically and have presented the growth rate (the imaginary part γ of Ω) in figure 1. We have taken the coupling constant $A_{\rm e} = 5$ and have assumed a two-dimensional ($D = 2$) geometry in the x–y-plane. The used mass ratio $m_{\rm h}/m_{\rm e} = 1$ is typical for light holes while $m_{\rm h}/m_{\rm e} = 5$ is typical for heavy holes [11]. We have taken the wavevectors $\mathbf{K}_{\rm e0}$ and $\mathbf{K}_{\rm h0}$ with opposite signs and directed along the x-axis, $\mathbf{K}_{\rm e0} = \widehat{\mathbf{x}}k_{\rm e0}$ and $\mathbf{K}_{\rm h0} = \widehat{\mathbf{x}}k_{\rm h0}$, where $\widehat{\mathbf{x}}$ is the unit vector in the x-direction. Hence, the electrons and holes are counter-streaming, and this gives rise to a streaming instability, as can be seen in figure 1. For the smaller wavenumber $|k_{\rm e0}| = |k_{\rm h0}| = 0.5\,\lambda_{\rm F}^{-1}$, the growth rate is smaller than for the larger wavenumber $|k_{\rm e0}| = |k_{\rm h0}| = 1.0\,\lambda_{\rm F}^{-1}$. Comparing the panels (a) and (b) with panels (c) and (d) of figure 1, we also see that the wave modes for the larger $|k_{\rm e0}|$ and $|k_{\rm h0}|$ have a wider spectrum of growing waves in oblique directions to the x-axis, while the wave modes for the smaller wavenumbers have growing wave modes primarily in the x-direction. When $k_{\rm e0}$ and $k_{\rm h0}$ are taken to be equal to each other, then the system is stable, i.e. the dispersion relation (7) has only real-valued roots in this case. In order to study the nonlinear saturation of the streaming instability, we have solved the time-dependent system of equations (1)–(3) numerically, and have presented the results in figure 2. As initial conditions we used $\psi_{\rm e} = n_0^{1/2}\exp({\rm i}k_{\rm e0}x)$ and $\psi_{\rm h} = n_0^{1/2}\exp({\rm i}k_{\rm h0}x)$,

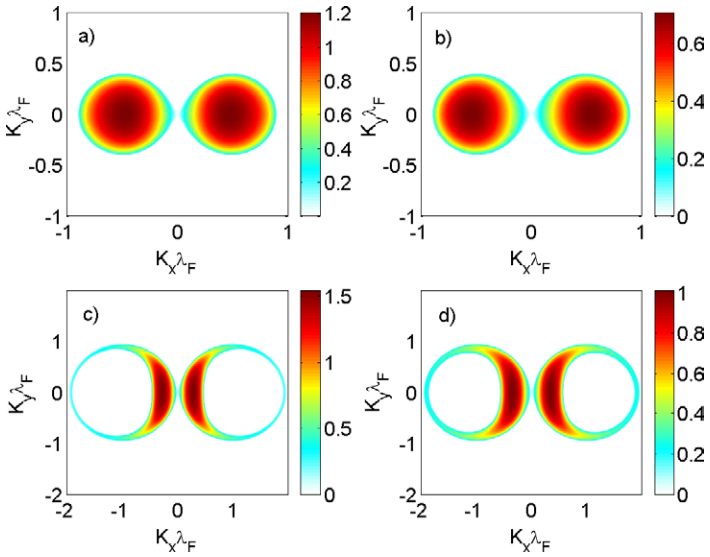

Figure 1. The growth rate γ (in units of t_F^{-1}) as a function of the wavenumbers K_x and K_y, for (a): $m_h/m_e = 1$, $k_{e0} = 0.5\,\lambda_F^{-1}$ and $k_{h0} = -0.5\,\lambda_F^{-1}$, (b): $m_h/m_e = 5$, $k_{e0} = 0.5\,\lambda_F^{-1}$ and $k_{h0} = -0.5\,\lambda_F^{-1}$, (c): $m_h/m_e = 1$, $k_{e0} = 1.0\,\lambda_F^{-1}$ and $k_{h0} = -1.0\,\lambda_F^{-1}$, and (d): $m_h/m_e = 5$, $k_{e0} = 1.0\,\lambda_F^{-1}$ and $k_{h0} = -1.0\,\lambda_F^{-1}$. We used $A_e = 5$ in all cases.

where we added a low amplitude noise (random numbers) of order $10^{-3}\,n_0^{1/2}$ to give a seed for any instability. We used the parameters in panel (d) of figure 1, i.e. the mass ratio $m_h/m_e = 5$ and wavenumbers $k_{e0} = 1.0\,\lambda_F^{-1}$ and $k_{h0} = -1.0\,\lambda_F^{-1}$. We see in figure 2 that density waves grow primarily in the x-direction, with a wavelength of $\lambda = 12\,\lambda_F$, corresponding to the wavenumber $K_x \approx 0.5\,\lambda_F^{-1}$ of the fastest growing wave in the upper right panel of figure 1. In the nonlinear stage, at $t = 12\,t_F$, very narrow density humps are formed at which both the electrons and holes are accumulated. At the later stage $t = 14\,t_F$, these density maxima break up into a chaotic pattern of very localized density patches. We see that the density maxima at all times are associated with a positive potential.

We next investigate the existence of two-dimensional ($D = 2$) vortex structures in our electron–hole system. Assuming that the electron and hole wavefunctions are in the form $\psi_e = \Psi_e(r)\exp(iM_e\theta - i\Omega_e t)$ and $\psi_h = \Psi_h(r)\exp(iM_h\theta - i\Omega_h t)$, where Ψ_e and Ψ_h are real-valued functions, r and θ are the polar coordinates defined by $x = r\cos\theta$ and $y = r\sin\theta$, Ω_e and Ω_h are constant frequency shifts and $M_e = 0, \pm1, \pm2, \ldots$ and $M_h = 0, \pm1, \pm2, \ldots$ are the different excited states (charge states) of the vortices, the system of equations (1)–(3) takes the form

$$\frac{\hbar^2}{2m_e}\left(\frac{d^2}{dr^2} + \frac{1}{r}\frac{d}{dr} - \frac{M_e^2}{r^2}\right)\Psi_e + (\hbar\Omega_e + e\phi - W_e)\Psi_e = 0, \tag{10}$$

$$\frac{\hbar^2}{2m_h}\left(\frac{d^2}{dr^2} + \frac{1}{r}\frac{d}{dr} - \frac{M_h^2}{r^2}\right)\Psi_h + (\hbar\Omega_h - e\phi - W_h)\Psi_h = 0, \tag{11}$$

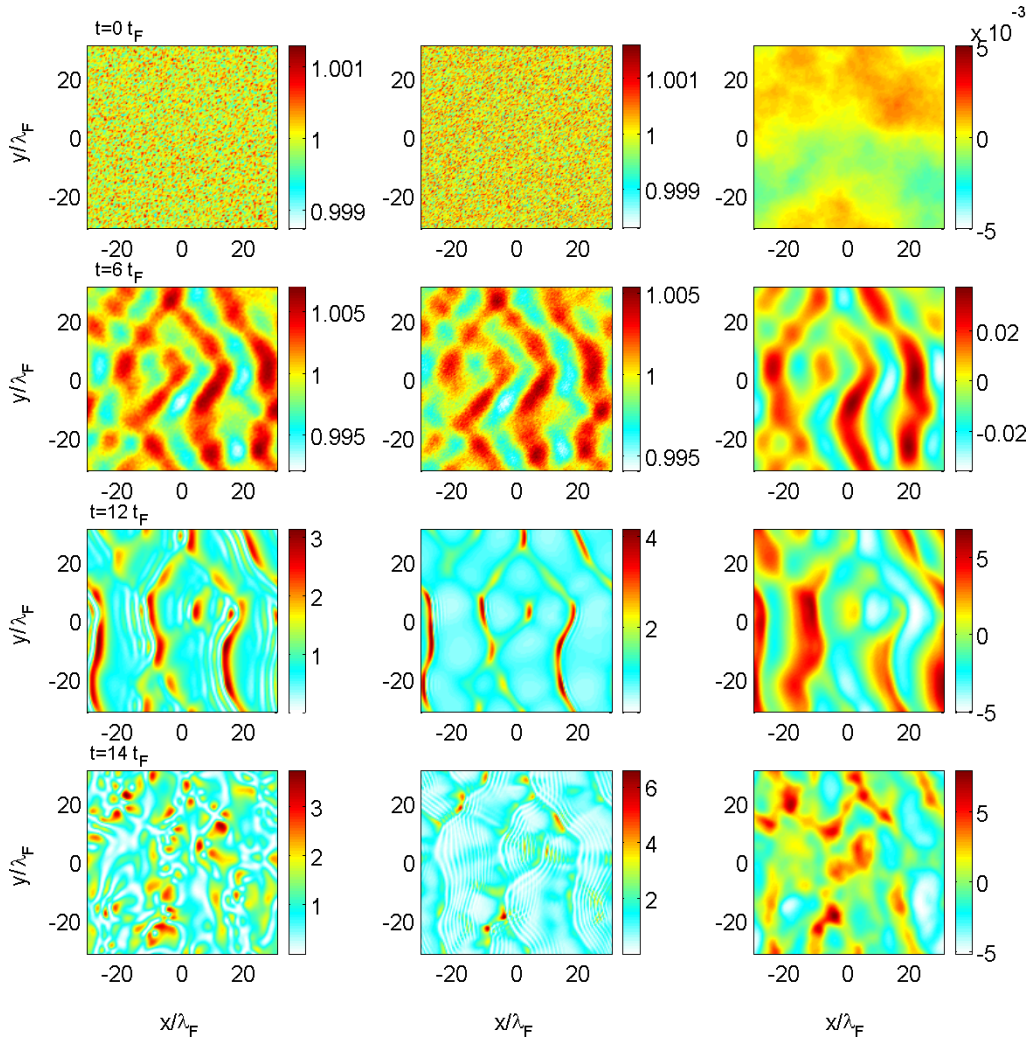

Figure 2. The electron number density (left column), hole number density (middle column) and potential (right column) at times $t = 0\,t_{\rm F}$, $6\,t_{\rm F}$, $12\,r_{\rm F}$ and $14\,t_{\rm F}$ for $m_{\rm h}/m_{\rm e} = 5$, $k_{\rm e0} = 1.0\,\lambda_{\rm F}^{-1}$, $k_{\rm h0} = -1.0\,\lambda_{\rm F}^{-1}$ and $A_{\rm e} = 5$. The number densities are normalized by n_0 and the potential ϕ by $T_{\rm Fe}/e$.

$$\left(\frac{{\rm d}^2}{{\rm d}r^2} + \frac{1}{r}\frac{\rm d}{{\rm d}r}\right)\phi = 4\pi e(|\Psi_{\rm e}|^2 - |\Psi_{\rm h}|^2). \tag{12}$$

For a localized structure, we have ${\rm d}/{\rm d}r = 0$, $\phi = 0$, $|\Psi_{\rm e}| = |\Psi_{\rm h0}| = n_0^{1/2}$ at $r = \infty$, and it follows that the frequency shifts take the forms $\Omega_{\rm e} = m_{\rm e}v_{\rm Fe}^2/2\hbar$ and $\Omega_{\rm h} = m_{\rm h}v_{\rm Fh}^2/2\hbar$. At $r = 0$, we have the boundary conditions ${\rm d}\Psi_{\rm e}/{\rm d}r = {\rm d}\Psi_{\rm h}/{\rm d}r = {\rm d}\phi/{\rm d}r = 0$, and it follows that $\Psi_{\rm e} = 0$ when $M_{\rm e} \neq 0$ and $\Psi_{\rm h} = 0$ when $M_{\rm h} \neq 0$. The numerical solutions of the system (10)–(12) are presented in figure 3 for a few sets of parameters. We see that the electron vortices with $M_x = 1$ show a complete depletion of the electrons in the centre of the vortex, while the hole vortices with $M_{\rm h} = 1$ are associated with a complete depletion of the holes. For a vortex with $M_{\rm e} = 1$ and $M_{\rm h} = 0$, we have a positive potential, while one with $M_{\rm e} = 0$ and $M_{\rm h} = 1$ has a negative potential. Finally, a vortex with equal charge states $M_{\rm e} = M_{\rm h} = 1$ has a zero potential, and in this case

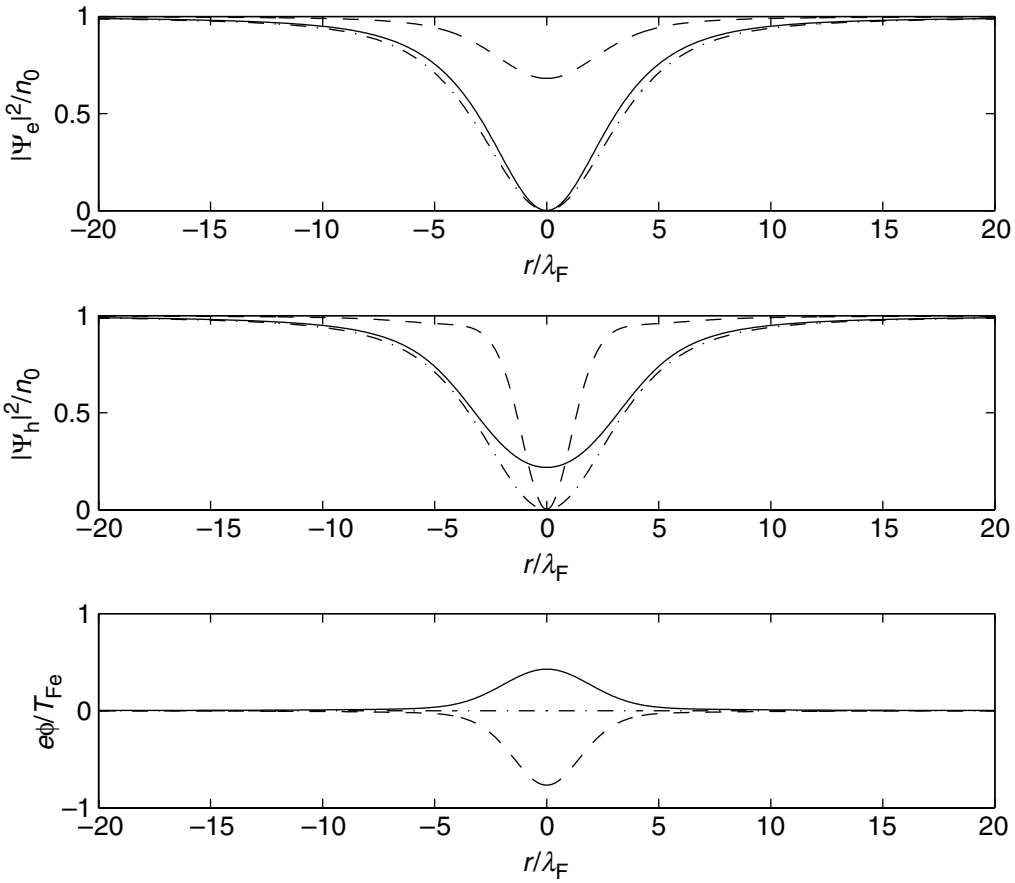

Figure 3. The electron number density (upper panel), hole number density (middle panel) and the potential (lower panel) for a two-dimensional vortex with the charge states $M_e = 1$ and $M_h = 0$ (solid lines), $M_e = 0$ and $M_h = 1$ (dashed lines) and $M_e = M_h = 1$ (dash-dotted lines). We used the parameters $A_e = 5$ and $m_h/m_e = 5$.

the system decouples completely into systems similar to those used to model BECs. In order to assess the dynamics and interaction between vortices, we have solved the time-dependent system (1)–(3) numerically, and as initial conditions we have used electron density perturbations in the form of vortex-like structures. The results are presented in figures 4 and 5. In figure 4, we used the initial condition $\psi_e = n_0^{1/2} f_1 f_2 f_3 f_4$, where $f_j = \tanh(\sqrt{(x - x_j)^2 + (y - y_j)^2}) \exp[+ iM_j \arg(x - x_j, y - y_j)]$. Here $(x_1, y_1) = (-4, 10)$, $(x_2, y_2) = (2, 10)$, $(x_3, y_3) = (-8, -10)$, and $(x_4, y_4) = (2, -10)$, and the charge states $M_1 = +1$, $M_2 = -1$, $M_3 = -1$ and $M_4 = +1$. The function $\arg(x, y)$ denotes the angle between the x-axis and the point (x, y), and it takes values between $-\pi$ and π. For the hole wavefunction we used the initial condition $\psi_h = 1$ everywhere. The initial condition for the electrons is such that the vortices are organized in two vortex pairs where the vortices in the vortex pair have opposite rotation polarities. Here the rotation polarities of the vortices are such that the two vortex pairs move in the direction against each other and collide, as seen at $t = 12\, t_F$ in figure 4. In the complicated interaction, the electron vortices dissolve and disappear, while there are instead two vortex pairs created in the hole fluid,

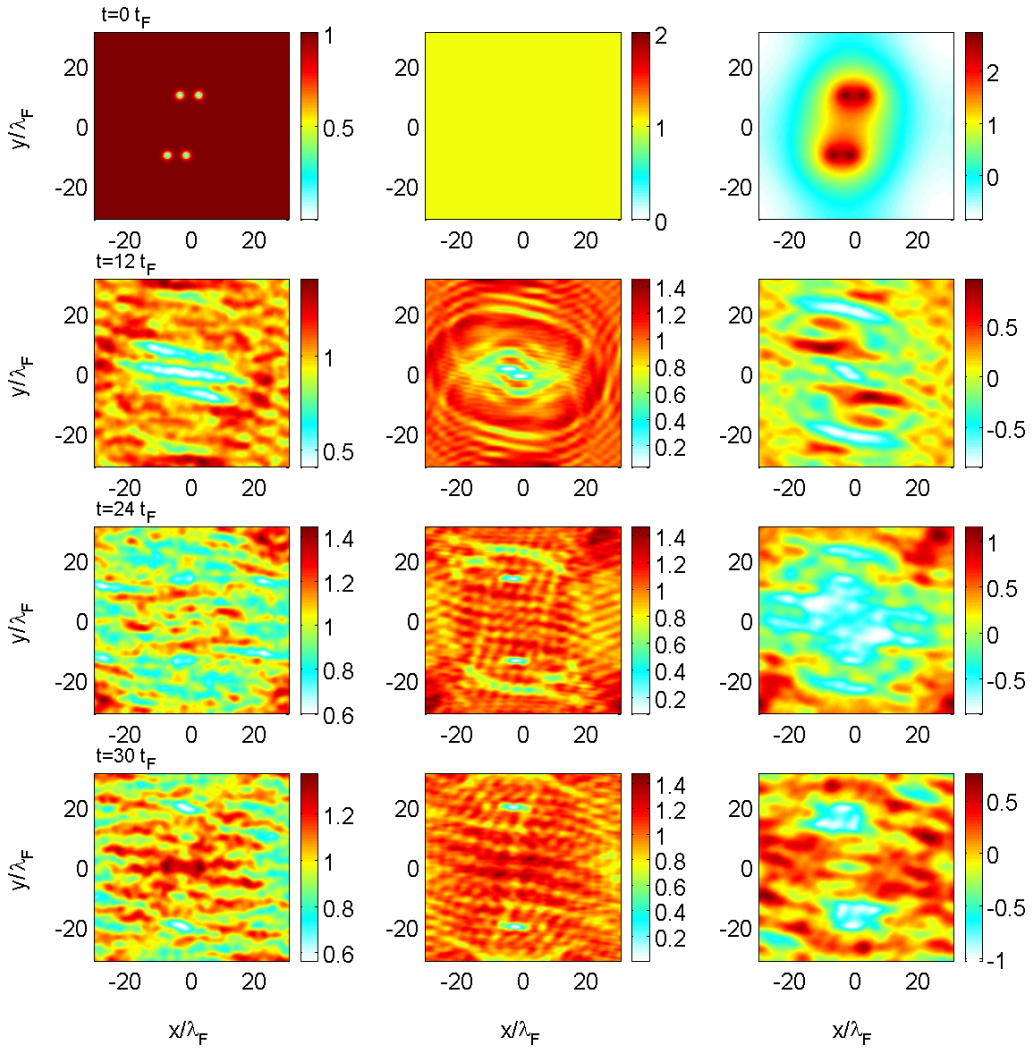

Figure 4. The electron number density (left column), hole number density (middle column) and the potential (right column) for two interacting vortex pairs at times $t = 0\,t_{\rm F}$, $12\,t_{\rm F}$, $24\,t_{\rm F}$ and $30\,t_{\rm F}$. We used the parameters $A_{\rm e} = 5$ and $m_{\rm h}/m_{\rm e} = 5$. The same normalization of variables as in figure 2 is used.

seen at $y \approx \pm 15\,\lambda_{\rm F}$ and $x \approx 0\,\lambda_{\rm F}$ at time $t = 24\,t_{\rm F}$ in figure 4. These hole vortex pairs have moved further to $y \approx \pm 20\,\lambda_{\rm F}$ at time $t = 30\,t_{\rm F}$ and are associated with a negative potential due to the sharp depletion of the hole density associated with the vortex pairs. In figure 5, we used the initial condition $\psi_{\rm e} = n_0^{1/2} f_1 f_2$, with $(x_1, y_1) = (-3, -20)\lambda_{\rm F}$ and $(x_2, y_2) = (3, -20)\lambda_{\rm F}$, and the charge states $M_1 = -1$ and $M_2 = +1$; see the top row of panels. Here, we see the formation of a quickly moving (in comparison with the hole vortex pairs in figure 4) electron vortex pair which moves towards positive y at $x = 0$. This vortex pair, which is located at $y = 20\,\lambda_{\rm F}$ at $t = 81\,t_{\rm F}$, is associated with a localized positive potential. We could also see the formation of a long-lived and slowly moving vortex pair in the hole fluid, seen at $y \approx -10\,\lambda_{\rm F}$ (and $x = 0\,\lambda_{\rm F}$) at $t = 8.1\,t_{\rm F}$, which is associated with a negative potential.

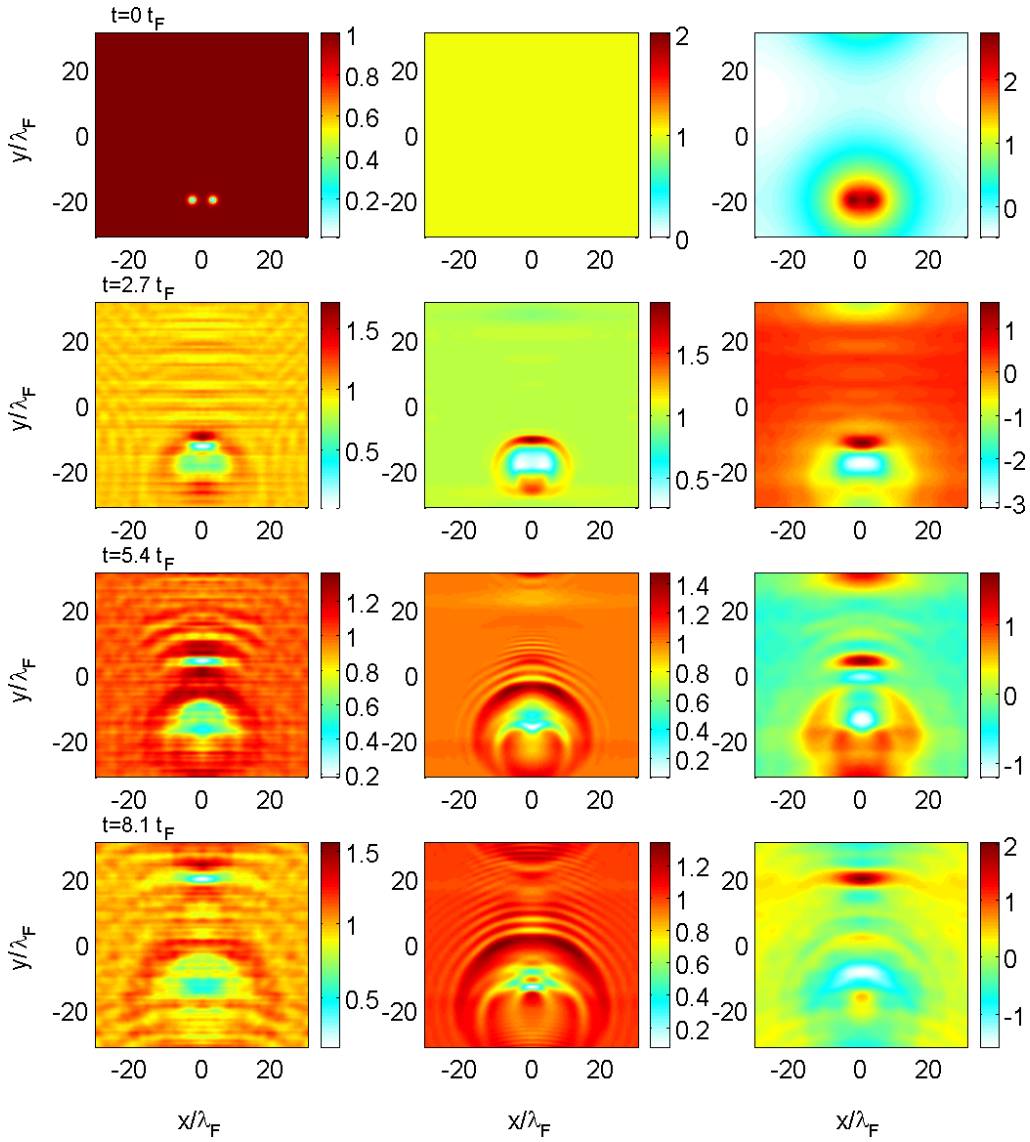

Figure 5. The electron number density (left column), hole number density (middle column) and the potential (right column) associated with a vortex pair at times $t = 0\,t_{\mathrm{F}}$, $2.7\,t_{\mathrm{F}}$, $5.4\,t_{\mathrm{F}}$ and $8.1\,t_{\mathrm{F}}$. We used the parameters $A_{\mathrm{e}} = 5$ and $m_{\mathrm{h}}/m_{\mathrm{e}} = 5$. The same normalization of variables as in figure 2 is used.

In conclusion, we have reported a new class of modulational instability and the formation of nonlinear structures in a polaritonic system. Our numerical analysis revealed the formation of electron and hole density humps (bright solitary waves) as possible nonlinear saturation of the modulational/streaming instability, while long-lived vortex pairs (dark solitons) can be excited in the electron–hole system via nonlinear interactions. Quantum vortices could be exploited to transport information at quantum scales in semiconductors and micromechanical devices, as well as in metal clusters [12].

References

[1] Markowich P A *et al* 1990 *Semiconductor Equations* (Berlin: Springer)
[2] Baranger H U *et al* 1993 *Chaos* **3** 665
[3] Berggren K-F and Ji Z-L 1996 *Chaos* **6** 543
[4] Opher M *et al* 2001 *Phys. Plasmas* **8** 2454
Marklund M and Shukla P K 2006 *Rev. Mod. Phys.* **78** 591
Chabrier G *et al* 2002 *J. Phys.: Condens. Matter* **14** 9133
[5] Becker K H, Schoenbach K H and Eden J G 2006 *J. Phys. D: Appl. Phys.* **39** R55
[6] Shpatakovskaya G V 2006 *JETP—Sov. Phys.* **102** 466
[7] Barnes W L *et al* 2003 *Nature* **424** 824
[8] Killian T C 2006 *Nature* **441** 297
[9] Kolomeisky E B *et al* 2000 *Phys. Rev. Lett.* **85** 1146
[10] Manfredi G and Haas F 2001 *Phys. Rev.* B **64** 075316
Manfredi G 2005 *Fields Inst. Commun.* **46** 263
[11] Kittel C 1996 *Introduction to Solid State Physics* (New York: Wiley) chapter 8
[12] Domps A *et al* 1998 *Phys. Rev. Lett.* **80** 5520